FRP REPAIR & STRENGTHENING OF DAMAGED END REGIONS OF PRESTRESSED BEAMS

Bassem Andrawes, Ph.D., Associate Professor, Department of Civil and Environmental Engineering, University of Illinois at Urbana-Champaign, Urbana, IL
Ian Shaw, Graduate Research Assistant, Department of Civil and Environmental Engineering, University of Illinois at Urbana-Champaign, Urbana, IL
Hang Zhao, Graduate Research Assistant, Department of Civil and Environmental Engineering, University of Illinois at Urbana-Champaign, Urbana, IL

ABSTRACT

A common serviceability problem in prestressed concrete (PC) bridges in the Midwest states is the deterioration/damage of the beams' end regions, which can be attributed to reasons like excessive thermal distortion in fascia beams or corrosion of steel reinforcement. Studies have shown that inadequate maintenance of expansion joints located at the beam end leads to excessive leakage of deicing materials and water onto the beam end, causing severe corrosion damage to shear reinforcement and also cracking and spalling of concrete. Another important factor that accelerates the rate of deterioration is the freeze-thaw cycles experienced by the concrete. To avoid the complete replacement of the beams with damaged ends, there is a need for effective repair measures that can restore/maintain the structural integrity and serviceability of these beams. This study focuses on exploring the effectiveness of conventional and innovative repairing methods to restore the shear capacity of PC beams with severely damaged end regions using experimental and numerical approaches. The use of Fiber Reinforced Polymer (FRP) laminates for repair was explored experimentally in addition to exploring numerically with FE modeling an innovative repair concept using prestressed Shape Memory Alloy (SMA) wires. Three half-scale PC I-girders are cast with reduced area stirrups in the end regions to represent damage. Various shear FRP laminate schemes are experimentally tested, including several which utilize longitudinal FRP strips to prevent premature laminate debonding from the concrete substrate. In the FE model curved prestressed SMA wires are embedded in the concrete cover to help restore the girder's shear strength.

Keywords: End region, Repair, Prestressed concrete, Fiber reinforced polymer, Shape memory alloy

INTRODUCTION

In the Northeast and Midwest of United States, over 58,000 bridges have been deemed structurally deficient and faced replacing, rehabilitation and repair[1]. Harsh climates in these regions caused deterioration in concrete structures at an accelerated rate. One specific problem that plagues bridges is the deterioration of the beam's end regions due to failure of expansion joint which allows water containing deicing salts to flow onto the beam ends, as shown in Figure 1(a). Another factor causing the damage at beam's end region is freezing and thawing cycles which result in scaling and spalling of the cover concrete. This does not only impact the appearance of the girders and increase the difficulty of inspection, but also directly expose the steel reinforcement to chlorides and accelerate the rate of corrosion of steel reinforcement and spalling of concrete. Due to the localized nature of this damage, the primary concern is shear failure. Traditionally mortar is utilized to repair girder's end region as shown in Figure 1(b). However, no studies were ever conducted to quantify the shear capacity gained by using mortar alone.

(a) (b)

Fig. 1 End region of prestressed girder: (a) end damage of girder; (b) typical mortar repair of girder end

Fiber reinforced polymer (FRP) laminates or sheets have been used as an effective repair and rehabilitation material over the past two decades because of its high strength to weight ratio and good corrosion resistance. One method of applying the laminates to the concrete surface is through a wet layup approach[2], in which the resin serves to saturate the fibers and bond the sheet to concrete surface. Due to its flexibility, FRP laminates could be added as external shear reinforcement to a girder through wet layup approach.

It has been proved that externally bonded FRP laminate could repair and strengthen the flexural behavior of concrete bridges[3,4,5,6]. More recently, externally bonded FRP in the form of U-wraps or bonded face plies has been proved to be effective in strengthening girders in shear[7]. However, there is limited studies focusing on the effectiveness of FRP repair combined with conventional mortar repair in short shear span.

This paper presents an experimental and numerical study on the application of FRP composites in repairing and retrofitting damaged ends of prestressed girders. Three-point bending tests were performed on small-scale girders repaired with mortar and FRP laminates systems. In addition, a full-scale girder finite element model was generated to explore the effectiveness of repair using FRP laminates and an innovative repair method using thermally-prestressed shape memory alloy (SMA) curved wires.

FLXURAL TESTING OF SMALL-SCALE GIRDERS

BEAM DESIGN AND CASTING

Three 23-ft (7-m) long small-scale PC beams were cast in the laboratory. The details of cross section and steel reinforcement are shown in Figure 2(a)-(c). The cross section of the beam was scaled to half size of AASHTO Type II I-girder and a top flange was cast on top to increase the flexural capacity of the beams. The compressive strength of the concrete at 28-day was 6.94 ksi (48.1 MPa). Three 0.5 in. (12.7 mm) diameter 7-wire strands with elastic modulus equal to 28700 ksi (197.9 GPa) and ultimate strength equal to 270 ksi (1862 MPa) were prestressed to 178 ksi (1234 MPa) (66% of ultimate strength). All the longitudinal and shear reinforcement had same yield strength equal to 60 ksi (414 MPa). At end region of the beam, the diameter of stirrups was reduced to 0.2 in. (5 mm) and spacing was increased to 5.0 in. (127 mm) to promote and facilitate shear failure.

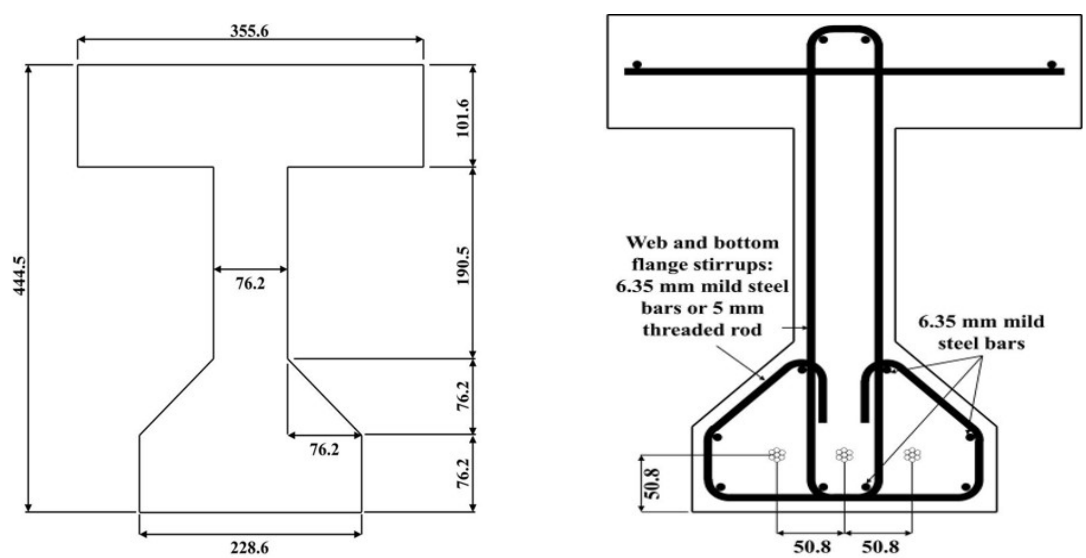

(a) (b)

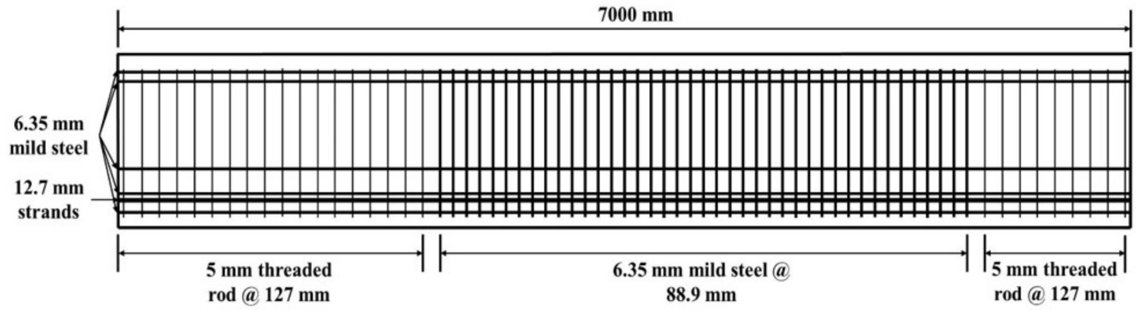

(c)

Fig. 2 Beam design (in mm): (a) cross section dimensions; (b) reinforcement details; (c) elevation view

TEST SETUP

Three-point bending tests were carried out to test the shear capacity of the beams. The test setup used is illustrated in Figure 3(a). To represent the localized nature of damage, a low span-to-depth ratio equal to 1.3 the beam's effective depth (d_p) was adopted. The depth to the prestressing strand (d_p) was 15.5 in. (394 mm), thus, the distance from the center of the support to the loading point was 20.0 in. (508 mm).

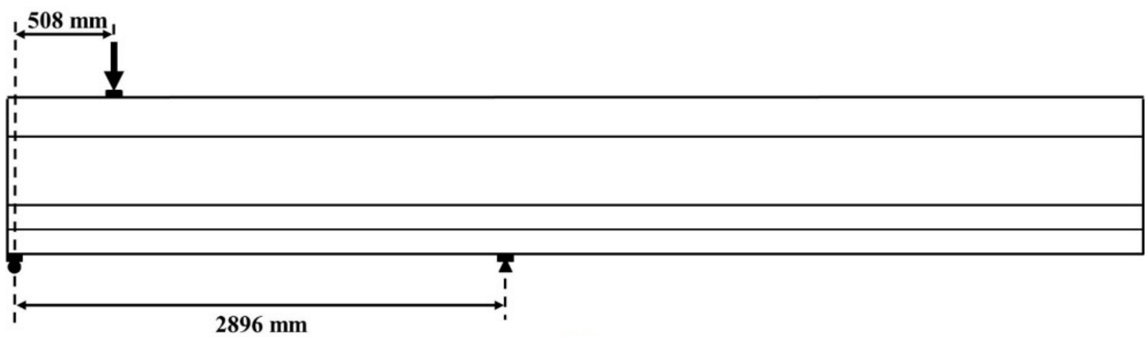

(a)

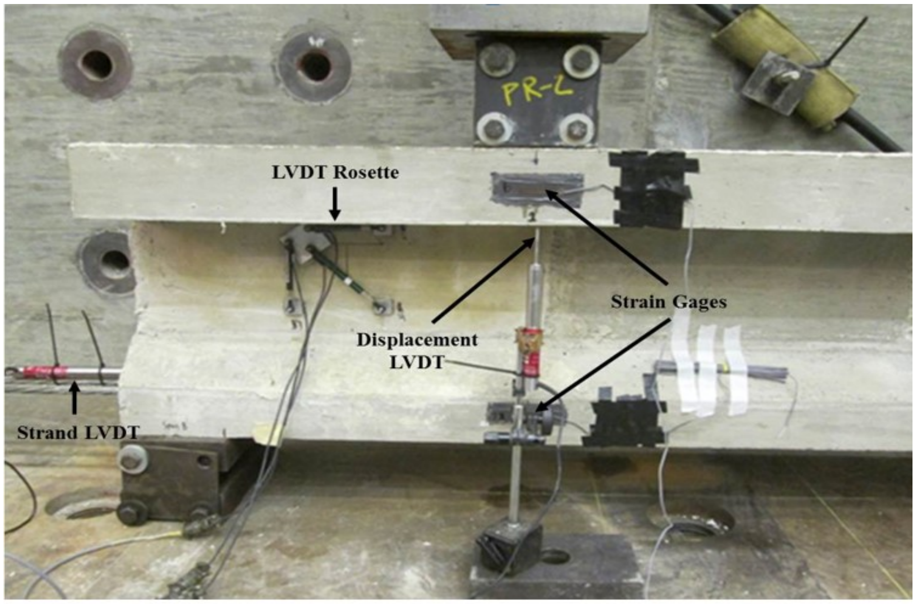

(b)

Fig. 3 Test setup: (a) three-point bending test; (b) beam instrumentation

The instrumentations used for the tests are shown in Figure 3(b). Three LVDTs placed at 0°, 45° and 90° formed a rosette configuration to measure the principal strain in the shear span. One vertical LVDT was placed beneath top flange to measure the deflection of the beam during loading. One LVDT was clamped to prestressing strand to monitor the end-slip of the strands. To measure compressive and tensile strains of the beam, two strain gages were attached to top and bottom flange of the beam. The test was controlled by displacement and load was applied by 100-kip (445-kN) capacity actuator.

DAMAGE AND REPAIR OF BEAM ENDS

The test matrix is shown in Table 1. There were five tests in total including control, damage, mortar repair and two FRP repair tests. The compressive strength of mortar used in repair is listed in the table.

Table 1. Test matrix

Test	**Cover Damage**	**Mortar Repair**	**FRP Repair**	**Mortar Compressive Strength, ksi (MPa)**
Control	--	--	--	--
Damaged	X	--	--	--
Mortar	X	X	--	3.39 (23.4)
GFRP	X	X	X	4.21 (29.0)
CFRP	X	X	X	3.99 (27.5)

To represent the damage to the end region of the girder in the field, removal of concrete cover with a depth equal to 0.5 in. (12.7 mm) was applied to the web within shear span on both sides. The beam web after removal of concrete cover is shown Figure 4.

Fig. 4 Beam web after cover removal

After cover was removed, the surface was vacuumed and air blasted. Afterwards a fast setting mortar was mixed and applied to the beam web. In addition to mortar repair, externally bonded glass-FRP (GFRP) and carbon-FRP (CFRP) laminates were also applied on the top of the cover mortar. The dimensions of FRP laminate systems used in test and the material properties are summarized in Table 2.

Due to the presence of bearing plate in the test and limited access to the bottom of the girder in the field, externally bonded U-wrap was not applicable. Thus, this study adopted bonded face ply FRP repair schemes. The FRP laminates started from the top of the beam web and terminated at the bottom edge of the bottom flange. Eight 6 in. (152.4 mm) wide panels of shear FRP reinforcement with vertical fiber orientation were attached to the beams using epoxy resin. Due to relatively low stiffness and strength of GFRP compared to CFRP, more plies of GFRP were utilized to achieve similar load in FRP for similar effective strain.

Table 2. Test matrix

Material	**Ply Thickness, in. (mm)**	**Shear Reinforcement Details**	**Elastic Modulus ksi, (GPa)**	**Tensile Strength ksi, (MPa)**	**Tensile strain, in./in. (mm/mm)**
GFRP laminate	0.050 (1.27)	8 x 6 in. (152.4 mm) x 3 plies	3219 (22.2)	57.8 (399)	0.018
CFRP laminate	0.049 (1.24)	8 x 6 in. (152.4 mm) x 1 ply	13300 (91.7)	147.9 (1020)	0.011

To improve the bond between FRP laminates and concrete, additional FRP strips were used as longitudinal anchors as shown in Figure 5(a). Three FRP strips were placed at the top of the web, bottom of the web and along the bottom edge of the bottom flange. To increase development of the anchors at beam end, the anchors were wrapped around beam end and continued along the other side. After laminates and anchors were attached, a strain gage was placed vertically on the FRP reinforcement close to the center of the shear span. Eventually repair using shear FRP reinforcement was shown in Figure 5(b).

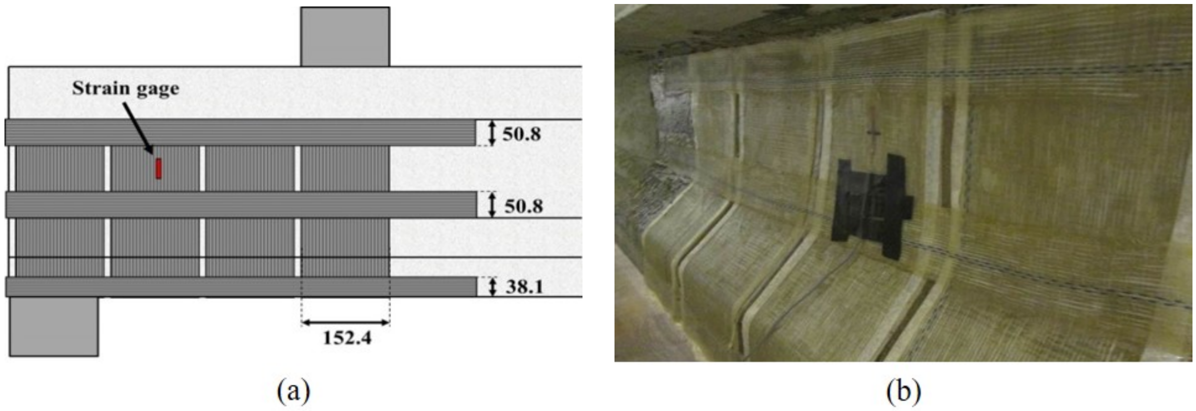

Fig. 5 FRP repair design: (a) FRP repair dimensions (mm); (b) FRP panels with longitudinal anchors

RESULTS AND DISCUSSION

The test results including peak load, secant stiffness at deflection equal to 0.079 in. (2 mm), slip of strand, max. principal strain and max. FRP strain are summarized in Table 3. The failure modes of the beams were governed by either shear cracking along the diagonal compression strut as in the cases of Control, Damaged, and Mortar specimens or debonding of FRP reinforcement as in the cases of GFRP and CFRP specimens. The load-deflection curves are depicted in Figure 6.

Table 3. Test results

Specimen	**Peak load, kips (kN)**	**% of Control peak load**	**% of Control stiffness**	**Strand slip at peak load, in. (mm)**	**Max. principal strain in web at peak load, in./in. (mm/mm)**	**Max. FRP strain, in./in. (mm/mm)**
Control	63.6 (282.9)	100.0	100.0	0.071 (1.81)	0.0153	--
Damaged	46.4 (206.4)	73.0	75.9	0.018 (0.46)	0.0063	--
Mortar	51.6 (229.5)	81.1	78.9	0.020 (0.51)	0.0062	--
GFRP	64.9 (288.7)	102.0	74.4	0.080 (2.03)	0.0108	0.0012
CFRP	76.0 (338.0)	119.5	106.0	0.052 (1.33)	0.0065	0.0034

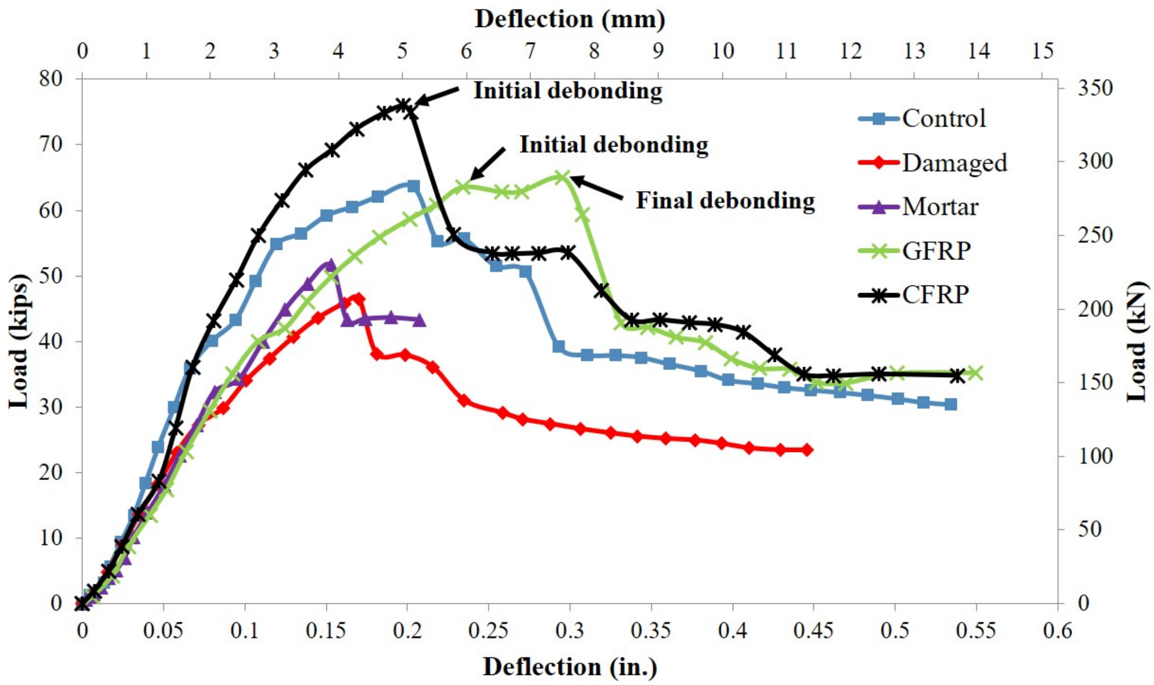

Fig. 6 Load-deflection curves

As shown in Figure 6, removal of concrete cover resulted in 27.0% and 24.1% reduction in peak load and stiffness respectively. Mortar repaired specimen reached 81.1% of the peak load and 78.9% of the stiffness of the Control specimen. The max. principal strain of Mortar specimen was lower than Control and Damaged specimen, which indicated that additional mortar didn’t fully engage with the core concrete. Two reasons could contribute to this issue: 1) the compressive strength of mortar was lower than that of beam concrete; 2) the cold joint existed between the exposed core concrete and mortar repair. At this interface, reduced aggregate interlock diminishes the strength recovery effect of the mortar repair. Such phenomenon is also suggested by the cracking patterns shown in Figure 7. The shear cracks of Control case propagate directly from the support to the loading plate while the shear cracks of Mortar case travel along the junction between web and bottom flange before proceeding up through the web.

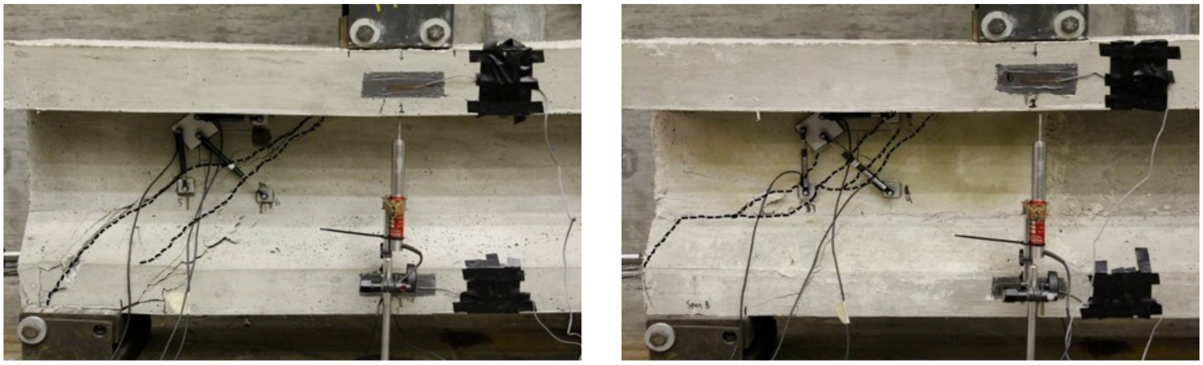

(a) (b)

Fig. 7 Shear crack patterns: (a) Control case; (b) Mortar repair case

With respect to FRP repair cases, both CFRP and GFRP repairs proven to be capable to restore the peak load of the beams. CFRP and GFRP tests reached 119.5% and 102.0% of the peak load of the Control test, respectively. However, only CFRP restored the stiffness of the beam, where CFRP test reached 106.0% of the stiffness of the Control specimen. The debonding patterns for both CFRP and GFRP are illustrated in Figure 8. From Figure 8(a), it is observed that in CFRP test debonding initiated in the endmost shear FRP panel and propagated further into adjacent panel. Due to the longitudinal anchors, complete delamination of CFRP laminates was prevented, as shown in Figure 8(b). While in GFRP test, debonding first occurred at web/bottom flange junction (see Figure 8(c)) and proceeded through the whole web and eventually complete debonding of GFRP sheets in second and third panels was observed (see Figure 8(d)). The ineffectiveness of the anchors in GFRP case can be attributed to the increased thickness of the shear FRP. Three plies of GFRP laminates reduced contact area between anchors and concrete in the 0.5 in. (12.7) mm gap between shear panels and sufficient bond was not provided to avoid complete delamination.

(a) (b)

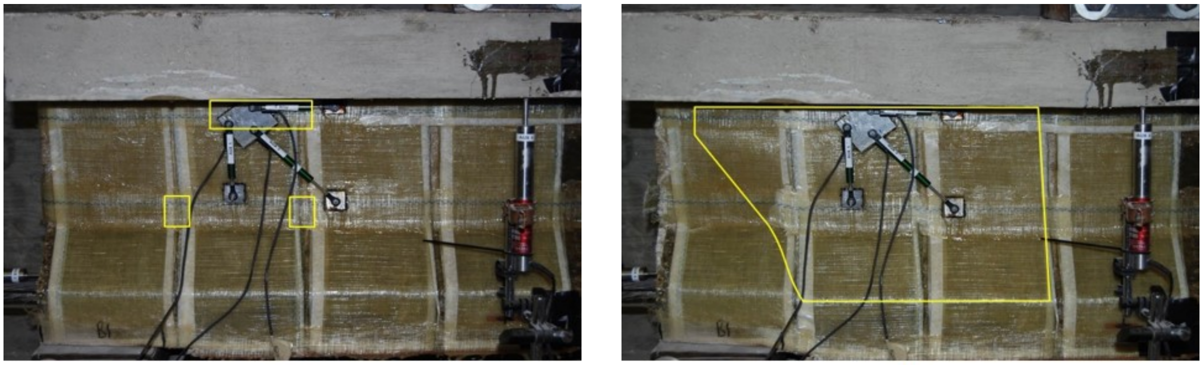

(c) (d)

Fig. 8 FRP laminates debonding patterns: (a) CFRP: initial debonding; (b) CFRP: final debonding; (c) GFRP: initial debonding; (d) GFRP: final debonding

FINITE ELEMENT ANALYSIS

MODEL DESCRIPTION AND CALIBRATION

A prestressed concrete (PC) I-girder from experimental tests performed by Andrawes and Pozolo[8] was utilized in the Finite Element Analysis (FEA) of this work[8]. The I-girder model included several geometrical parts: high strength prestressed strands, mild steel rebars and stirrups, concrete girder and loading/support plates. The details of the cross section of the PC I-girder is depicted in Figure 9. To reduce computational demand, only half of the I-girder cross section is modeled with a symmetric boundary condition defined on the inner face of the girder. Details about size and location of mild steel rebars and stirrups could be found in Andrawes and Pozolo's work[9].

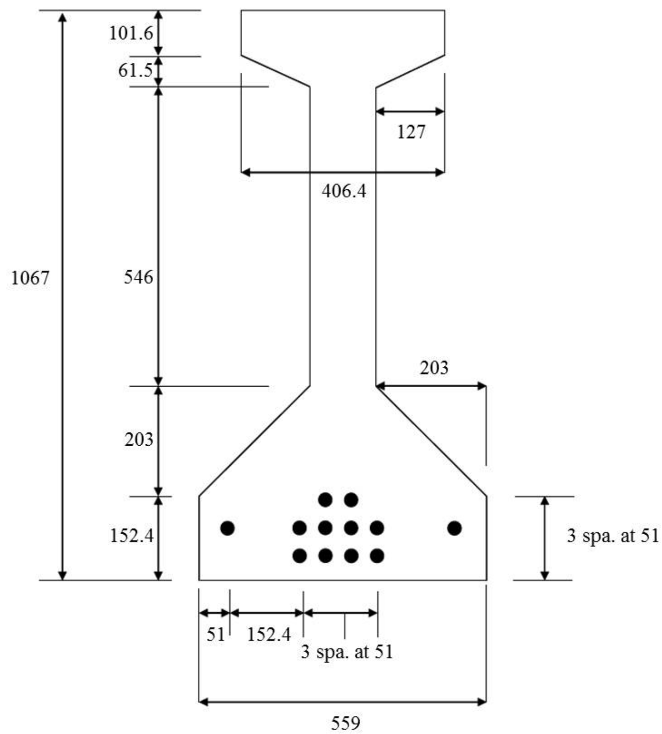

Fig. 9 Cross section of I-girder, in mm

The mild steel rebar and stirrups have a yield strength of 60 ksi (413.8 MPa) and elastic modulus of 29000 ksi (200 GPa). The high strength prestressed strands have a cross section of 0.153 in.^{2} (98.7 mm^2), with elastic modulus equal to 28700 ksi (197.9 GPa) and ultimate strength equal to 270 ksi (1862 MPa). The mild steel rebars and stirrups and prestressing strands were modeled using T3D2 2-node linear 3-D truss elements because those elements are only subjected to tension and compression. Prestressing was applied to the strands by imposing a negative predefined temperature field and the thermal expansion coefficient was chosen so that an effective prestress reached approximately 165 ksi (1140 MPa). The concrete has a compressive strength equal to 6.06 ksi (41.8 MPa). The support/loading plates have the same material property as the mild steel. Both concrete girder and support/loading plates were modeled using C3D8 8-nodel linear brick elements.

A three-point bending test was performed using the same test setup of Test 7 in Andrawes and Pozolo's work[8], which has a shear span of 57.9 in. (1.47 m) and a support-to-support distance of 427 in. (10.84 m). The test setup and model assembly are illustrated in Figure 10. The deflection was measured under the point of loading. The load-deflection curve is shown in Figure 11. Although the FE model showed slightly higher initial stiffness than test result, the load-deflection curve showed relatively good match.

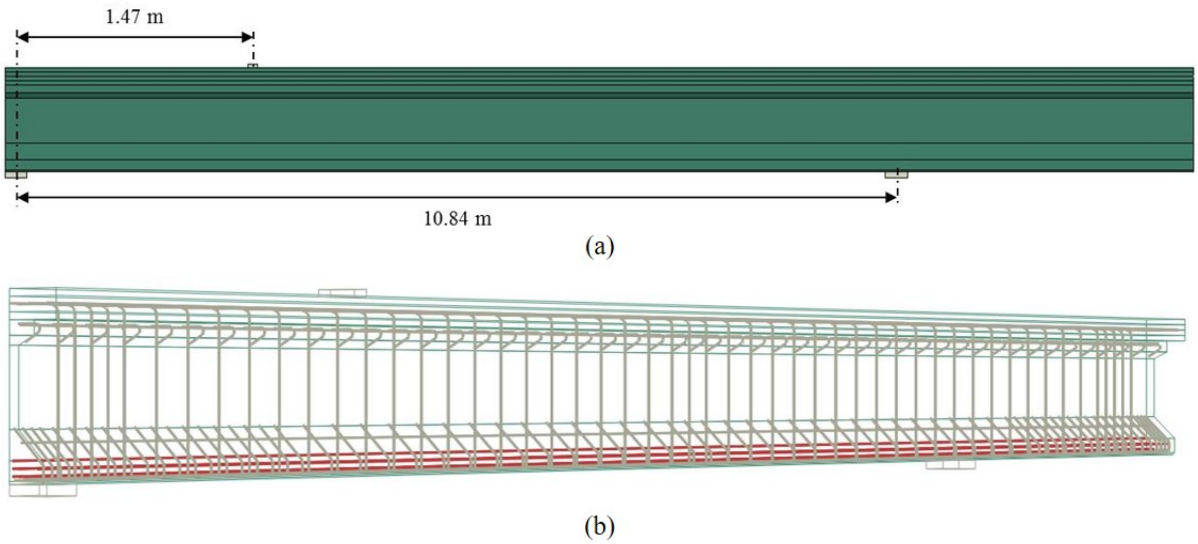

Fig. 10 Model assembly: (a) Test setup of three-point bending test; (b) view of internal reinforcement

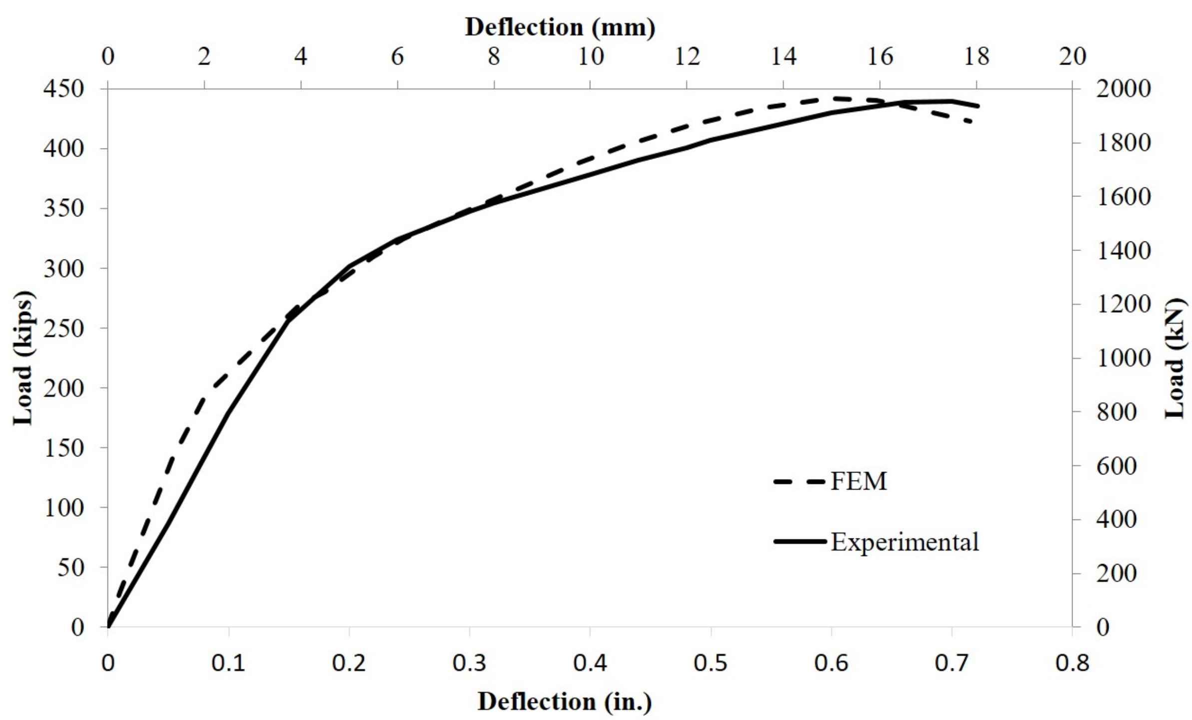

Fig. 11 Load-deflection curve

DAMAGE AND REPAIR ANALYSIS

The damage to the beam end is mainly governed by the cracking/spalling of concrete cover and corrosion of steel reinforcement. To simulate these damages, both the concrete property of web cover and steel property of stirrups are reduced. Damage progression is adopted to represent the real damage situation in the field, which is the region away from beam end experienced less severe damage. As shown in Figure 12(b), the concrete cover within shear span is divided into three 20 in. (508 mm) regions and had different properties. The region (Zone 1) close to the beam end has 0.0f'$_c$. 0.2f'$_c$ and 0.5f'$_c$ are assigned to Zone 2 and Zone 3 respectively. Figure 12 (d) illustrates the damage progression for vertical stirrups.

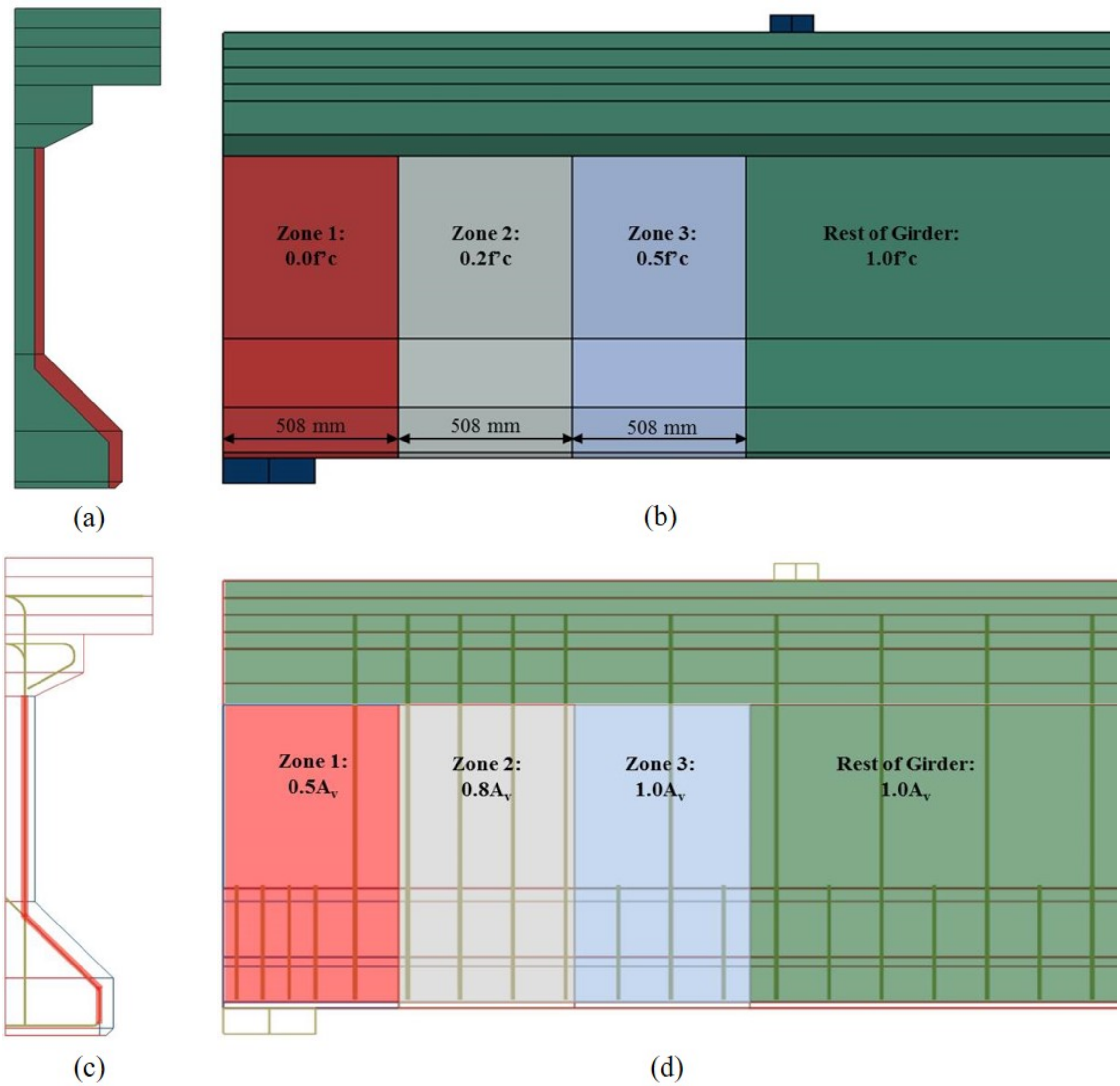

Fig. 12 Progressive end region damage scheme: (a) cover damage profile; (b) cover damage zones; (c) stirrups damage profile; (d) stirrups damage zones

After the damage is introduced, repair technique is applied. The first repair case is repair using mortar only. The compressive strength of mortar in early set stage tends to be in the range of 2.9-4.35 ksi (20-30 MPa) and the cold joint between mortar and existing concrete might diminish the contribution of mortar to restore the shear capacity of the girder. Thus, the strength of mortar used in the model was approximately 3.03 ksi (20.9 MPa). As a result, the cover concrete strength of Zone 1 and Zone 2 is increased to 0.5f'$_c$ while the cover concrete strength of Zone 3 remains the same.

In addition to mortar repair, two FRP repair systems consisting of externally bonded FRP laminates and prestressed SMA wires are investigated in this study. Due to its high strength, CFRP laminate is utilized as additional shear reinforcement. One ply of CFRP laminate covered the whole three damaged zones within shear span. The bond between shear FRP reinforcement and mortar is simulated by using COH3D8 8-node three-dimensional cohesive element. Additional two longitudinal strips with width equal to 3 in. (76 mm) serve as anchors to improve the bond between sheet and mortar and delay the delamination. A bond length of 2 in. (51 mm) at beam end and 6 in. (152 mm) extension past shear panel would ensure sufficient development of those. Repair with externally bonded CFRP laminates are shown in Figure 13. Properties for CFRP composite are from manufacturer's data[10].

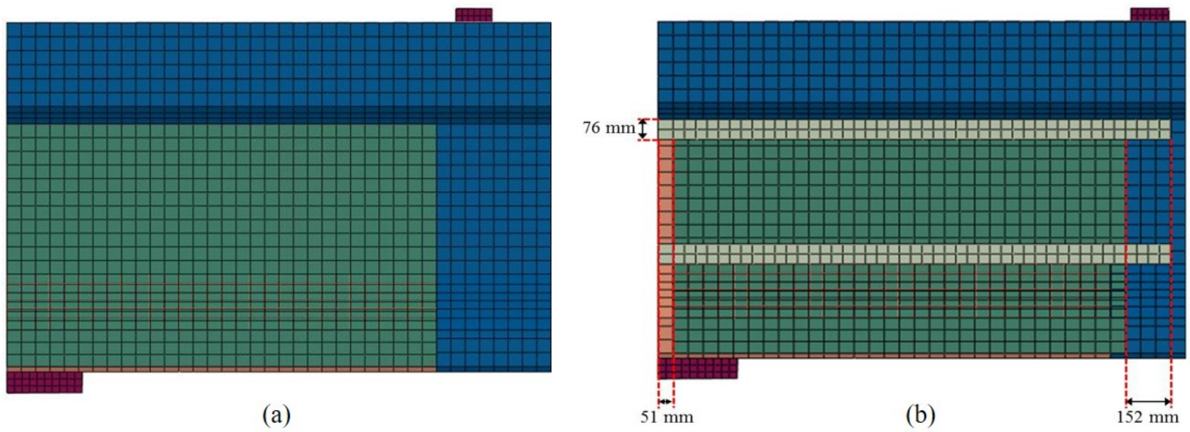

Fig. 13 CFRP repair scheme: (a) CFRP (Zone 1 to Zone 3); (b) CFRP-wa (with anchors)

To address the concern which many bridge engineers express regarding recovery of the already distressed regions of the beam with external FRP laminates, which makes future inspection quite difficult, a new repair approach using embedded prestressed wires was explored numerically. Due to the ease and low labor required for prestressing shape memory alloy (SMA) wires[11], they were considered in this exploratory study. As illustrated in Figure 14, previous studies showed that 0.079 in. (2 mm) -diameter SMA wire with 6.2% prestrain could produce considerable recovery stress (prestress) simply through heating. This prestress will be maintained at a wide range of ambient temperature.

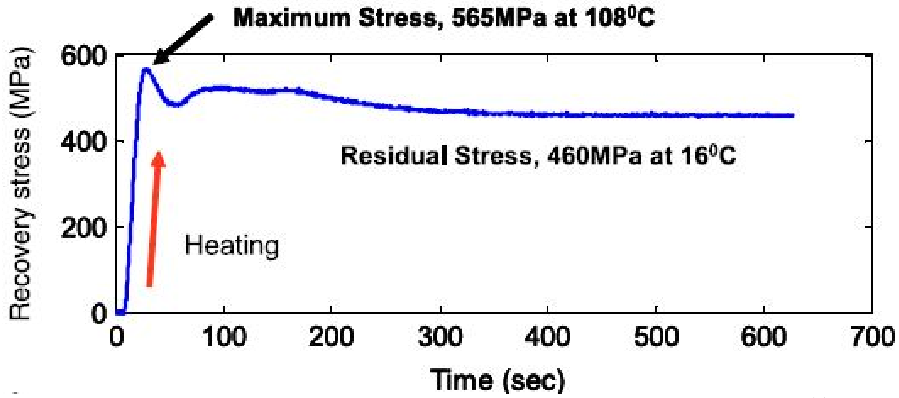

Fig. 14 Recovery stress developed in SMA during heating[11]

By making use of this unique characteristic of SMA, embedding small diameter curved SMA wires (see Figure 15) into concrete cover of the short shear span region would generate sufficient stress in the web to improve the stiffness and shear strength and to control the crack propagation in this relatively limited-space region. Curved SMA wire with 18 in. (457 mm) straight legs are embedded. The SMA wire has cross section area of 0.098 in.^{2} (63.2 mm^2) (20 wires of 0.079 in. (2 mm) diameter) and spacing of 4 in. (102mm), which is approximately 23% of strength-wise equivalent area of CFRP laminate. Another case with same spacing and section area of 0.049 in.^{2} (31.6 mm^2) (10 wires of 0.079 in. (2 mm) diameter), which is approximately 12% of strength-wise equivalent area of CFRP laminate, is also explored.

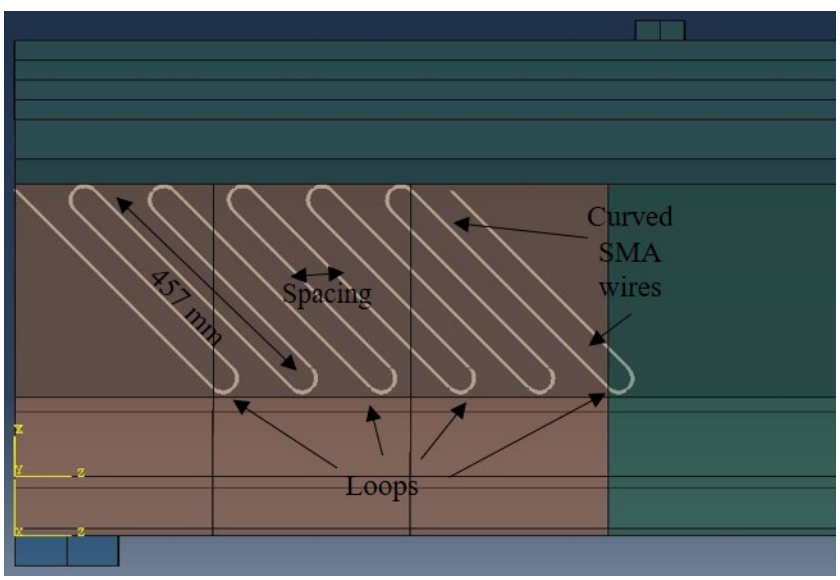

Fig. 15 Prestressed SMA repair

RESULTS AND DISCUSSION

The numerical results including peak load, secant stiffness at deflection equal to 0.197 in. (5 mm) were summarized in Table 4. The load-deflection curve for mortar repair and CFRP repair is illustrated in Figure 16.

Table 4. Finite element analysis results

Specimen	Peak load, kips (kN)	% of Control peak load	% of Control stiffness
Control	435.2 (1935.8)	100.0	100.0
Damaged	341.5 (1518.9)	78.5	88.9
Mortar	366.3 (1629.4)	84.2	94.4
CFRP	446.0 (1983.7)	102.5	97.3
CFRP-wa	459.4 (2043.5)	105.6	97.6
SMA-20	477.1 (2122.1)	109.6	121.5
SMA-10	434.4 (1932.3)	99.8	114.9

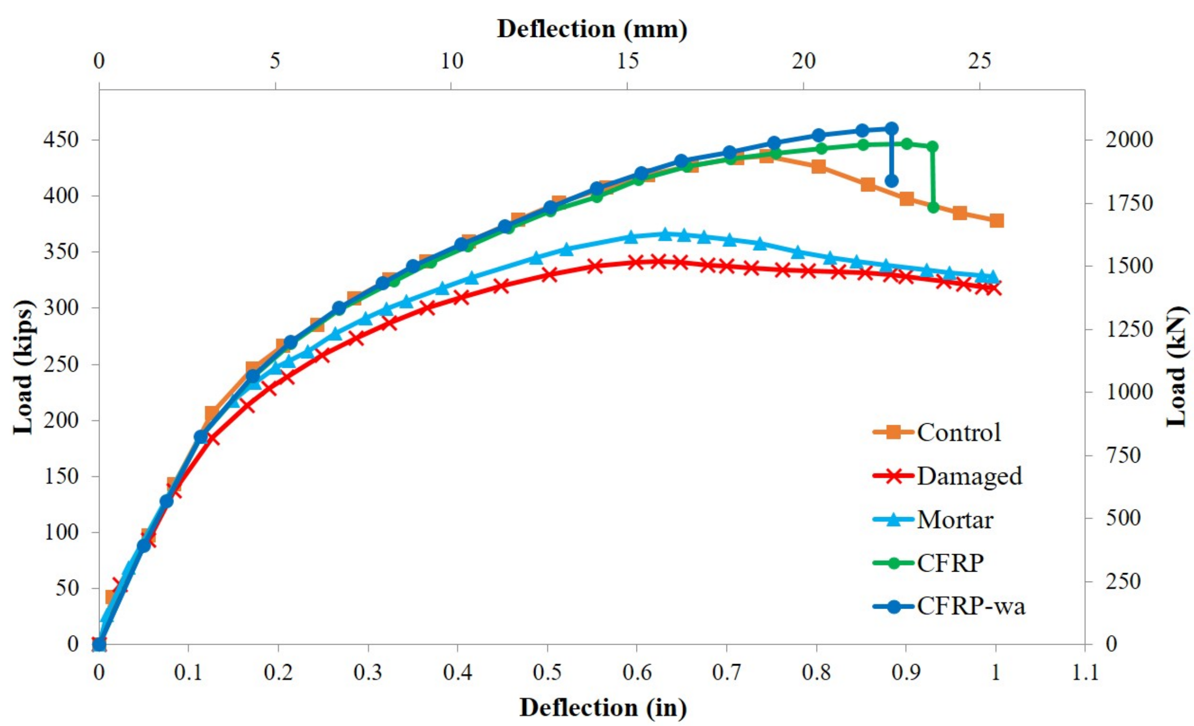

Fig. 16 Load-deflection curve of FRP repair cases

From the figure, it is shown that mortar repair only showed 5.7% increase in peak force and 5.5% increase in stiffness compared to damaged case, indicating that mortar alone is not sufficient to restore the capacity of the girder. Both CFRP case and CFRP with anchor case recovered the shear capacity of the girder. The peak force is increased by 24.0% and 27.1% for CFRP and CFRP-wa, respectively. Compared to CFRP case, CFRP repair with longitudinal anchors showed 3.1% increase in peak force and proved the effectiveness of strip anchors.

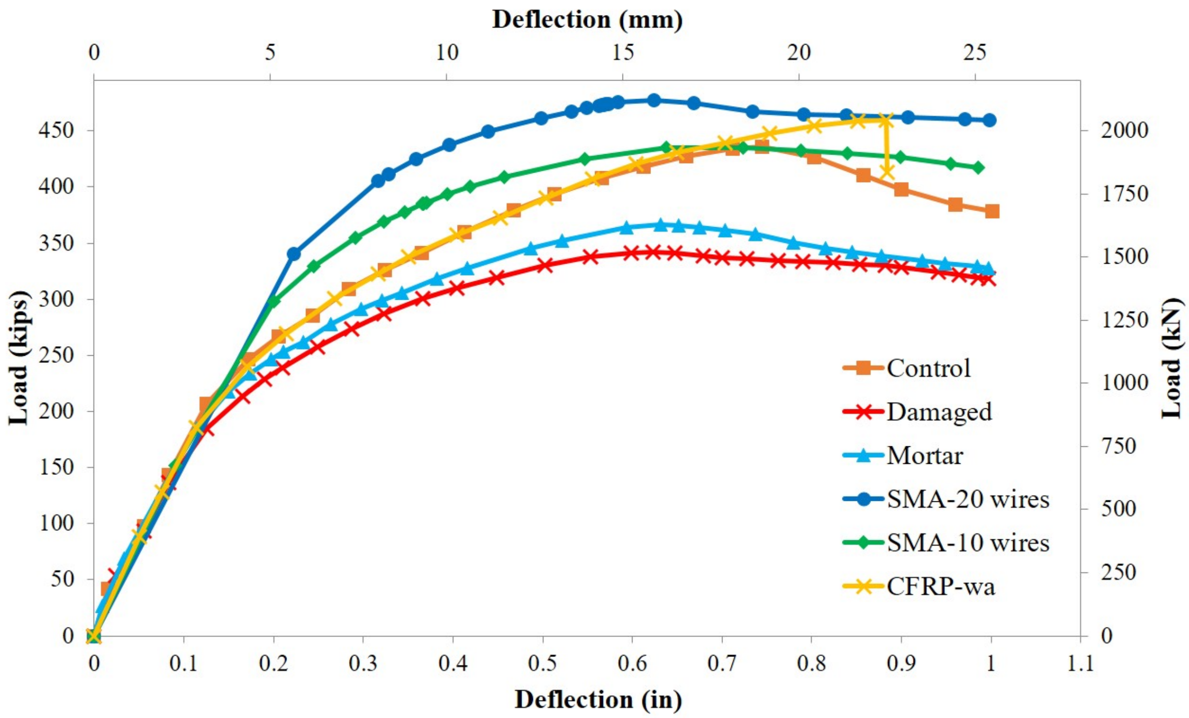

Fig. 17 Load-deflection curve of FRP and prestressed SMA repairs

Load-deflection curve of prestressed SMA repair is illustrated in Figure 17. From the curves, it is observed that both SMA repair cases restored the peak force of the girder. More importantly, compared to control case the stiffness is increased by 21.5% and 14.9% for 20 wires case and 10 wires case, respectively. The stiffness is even higher than that of CFRP-wa repair. This is because the SMA prestressing was effectively able to delay the development of shear cracks in the web. The results indicate that applying prestressing in the web is effective in regaining strength and stiffness of the girder with end damage.

CONCLUSIONS

In this study, three-point bending tests were performed on prestressed beams with damaged ends. Repair with mortar alone and mortar combined with externally bonded FRP laminates was conducted. A FE model of a full-scale prestressed I-girder was generated using different repair schemes were also explored. Based on the experimental and numerical results above, it is shown that a mortar repair alone is not sufficient to regain the strength and stiffness of girders with severely damaged ends. With additional externally bonded shear FRP sheets, the shear capacity of the prestressed girder with damaged end could be restored. Longitudinal anchors have been proven to be effective in preventing complete delamination of FRP laminates. To increase the effectiveness of GFRP repair, a stronger anchorage system is needed. From numerical results, it was shown that embedded prestressed SMA wires were effective in repairing the damaged end, especially in increasing the stiffness of the damaged girder.

REFERENCES

1. ARTBA, http://www.artba.org/economics/2016-u-s-deficient-bridges/, 2016.
2. Alkhrdaji, T., "Strengthening of Concrete Structures Using FRP Composites", *STRUCTURE magazine*, June 2015.
3. Tedesco, J.W., Stallings, J.M., and EL-Mihilmy, M., "Rehabilitation of a Reinforced Concrete Bridge Using FRP Laminates", RP 930-341; Highway Research Center, Auburn University, Auburn, AL, 1998.
4. Nanni, A., "Strengthening of an Impact-Damaged PC Girder," *Concrete Repair Bulletin*, May-June 2004.
5. Carmichael, B.M., and Barnes, R.W., "Repair of the Uphapee Creek Bridge with FRP Laminates", RP 930-466; Highway Research Center, Auburn University, Auburn, AL, 2005.
6. ElSafty, A., and Graeff, M.K., "The Repair of Damaged Bridge Girders with Carbon-Fiber-Reinforced Polymer "CFRP" Laminates", BDK82 977-03; School of Engineering, University of North Florida, Jacksonville, FL, 2012.
7. Belarbi, A., Bae, S., Ayoub, A., Kuchma, D., Mirmiran, A., and Okeil, A., "Design of FRP Systems for Strengthening of Concrete Girders in Shear," Research Report No. 678; NCHRP, 2011.
8. Abaqus 6.13, SIMULIA by Dassault Systèmes, software available at https://www.3ds.com.
9. Andrawes, B., and Pozolo, A., "Transfer and Development Lengths in Prestressed Self-consolidating Concrete Bridge Box and I-girders", Research Report No. ICT-11-092; University of Illinois at Urbana-Champaign, Urbana, IL, USA, 2011.
10. QuakeWrap, "Product Data Sheet: QuakeWrap TU27C Carbon Fabric for Structural Strengthening," QuakeWrap Inc.; Tucson, AZ, USA, 2016.
11. Shin, M., and Andrawes, B., "Experimental Investigation of Actively Confined Concrete Using Shape Memory Alloys," *Engineering Structures*, V. 32, No. 3, November 2009, pp. 656-664.